

Isolation and characterization of non-sulfated and sulfated triterpenoid saponins from *Fagonia indica*

Nayab Kanwal^a, Achyut Adhikari^a, Abdul Hameed^b, Rahman M. Hafizur^b, Syed Ghulam Musharraf^{a,*}

^a H.E.J. Research Institute of Chemistry, International Center for Chemical and Biological Sciences, University of Karachi, Karachi, 75270, Pakistan

^b Dr. Panjwani Center for Molecular Medicine and Drug Research, International Center for Chemical and Biological Sciences (ICCBS), University of Karachi, Karachi, 75270, Pakistan

ARTICLE INFO

Article history:

Received 9 May 2017

Received in revised form

3 August 2017

Accepted 7 August 2017

Keywords:

Fagonia indica

Zygophyllaceae

Triterpenoid glycosides

Insulin secretion activity

ESI-QTOF-MS

ABSTRACT

Seven previously undescribed, sulfated triterpenoid glycosides, named nayabin A-G along with a known triterpenoid glycoside were isolated from the whole plant of *Fagonia indica*. Their structures were elucidated through spectral studies including 1D- (¹H and ¹³C), 2D-NMR spectroscopy (HSQC, HMBC, COSY and NOESY), and mass spectrometry (ESI-MS/MS). β -D-Glucopyranosyl 3 β -hydroxy-23-O- β -D-glucopyranosyloxy-taraxast-20-en-28-oate, a known compound exerts glucose-dependent insulin secretory activity, which seems to exhibit a decreased risk of drug-induced hypoglycemia and may offer distinct advantages as anti-diabetic agent.

© 2017 Elsevier Ltd. All rights reserved.

1. Introduction

Fagonia indica Burm belongs to family Zygophyllaceae. It is small spiny shrub, very much branched desert herb up to 80 cm tall and widely distributed in tropical, subtropical, and warm areas of the world. It is also present in dry areas. Algeria, Cyprus, Egypt, India, Morocco, Pakistan, Saudi Arabia are known countries for this plant occurrence (Ali et al., 2008). This plant has saponin or triterpenoid glycoside rich constituents. *Fagonia* species are often used in traditional medicines, such as for treatment of fever, jaundice (Hammiche and Maiza, 2006), blood purification, cold, cough (Khattak, 2012), asthma, skin infection, liver problems (Abirami et al., 1996), carminative, emetic (Mahmood et al., 2011), and the extracts of these plants have been reported to exhibit anti-microbial, anti-inflammatory, analgesic and antipyretic activities (Nagaraj and Venkateswarlu, 2013; Sajid et al., 2011; Thetwar et al., 2006). Additionally, this plant is declared to be remedy for cancer (Hussain et al., 2007; Satpute et al., 2009; Waheed et al., 2012) and thalassemia (Seyal et al., 2013). The medicinal properties of this

plant were attributed due to its variety of active phytochemical constituents. A large number of saponins or triterpenoid glycosides (Abdel-Khalik et al., 2001; Ansari et al., 1987; El-Wakil, 2007; Farheen et al., 2015; Khalik et al., 2000; Miyase et al., 1996; Shaker et al., 1999, 2013) have been isolated and characterized from various species of *Fagonia*. Sulfated triterpenoids and sulfated triterpenoid glycosides have been isolated from *Fagonia* species (Perrone et al., 2007; Shaker et al., 2000). Saponins are considered as the major bioactive constituents of the drugs, mainly used for their haemolytic (Amini et al., 2014), anti-inflammatory (Lee et al., 2012), anti-microbial (Lunga et al., 2014), and antitumor (Han et al., 2013) activities. Some saponins from *Fagonia* species have been reported to exert anti-cancer, anti-diabetic, molluscicidal and antioxidant activities (El-Wakil, 2007; Farheen et al., 2015; Saleem et al., 2014; Shaker et al., 2013).

The medicinal importance of *Fagonia* encouraged us to investigate the saponins in *Fagonia indica*. This paper reports the isolation and characterization of seven previously undescribed including triterpenoid glycosides (1, 3), five sulfated triterpenoid glycosides (2, 4–7) and a known triterpenoid glycoside (8). Their structures were elucidated by extensive spectroscopic methods including 1D- (¹H and ¹³C) and 2D-NMR (COSY, HSQC, HMBC, and NOESY) experiments as well as ESI-MS and ESI-MS/MS analysis. To elucidate

* Corresponding author.

E-mail address: musharraf1977@yahoo.com (S.G. Musharraf).

the importance of these isolated compounds, we have evaluated these natural compounds for their insulin secretory activity in *in vitro* isolated mice islets and cytotoxicity activities in MIN6 cell lines.

2. Results and discussion

The n-BuOH fraction obtained from the extract (MeOH/H₂O:

8/2) of the whole plant of *Fagonia indica* was fractionated by vacuum-liquid chromatography (VLC) using reversed phase silica gel (C18) followed by column chromatography (silica gel) and recycling HPLC, to afford seven previously undescribed triterpenoid saponins (**1–7**) and one known triterpenoid saponin (**8**) (See Fig. 1). Spectral analysis indicated that compounds **1**, **3**, **8** are non-sulfated triterpenoid saponins and compounds **2**, **4–7** are sulfated triterpenoid saponins.

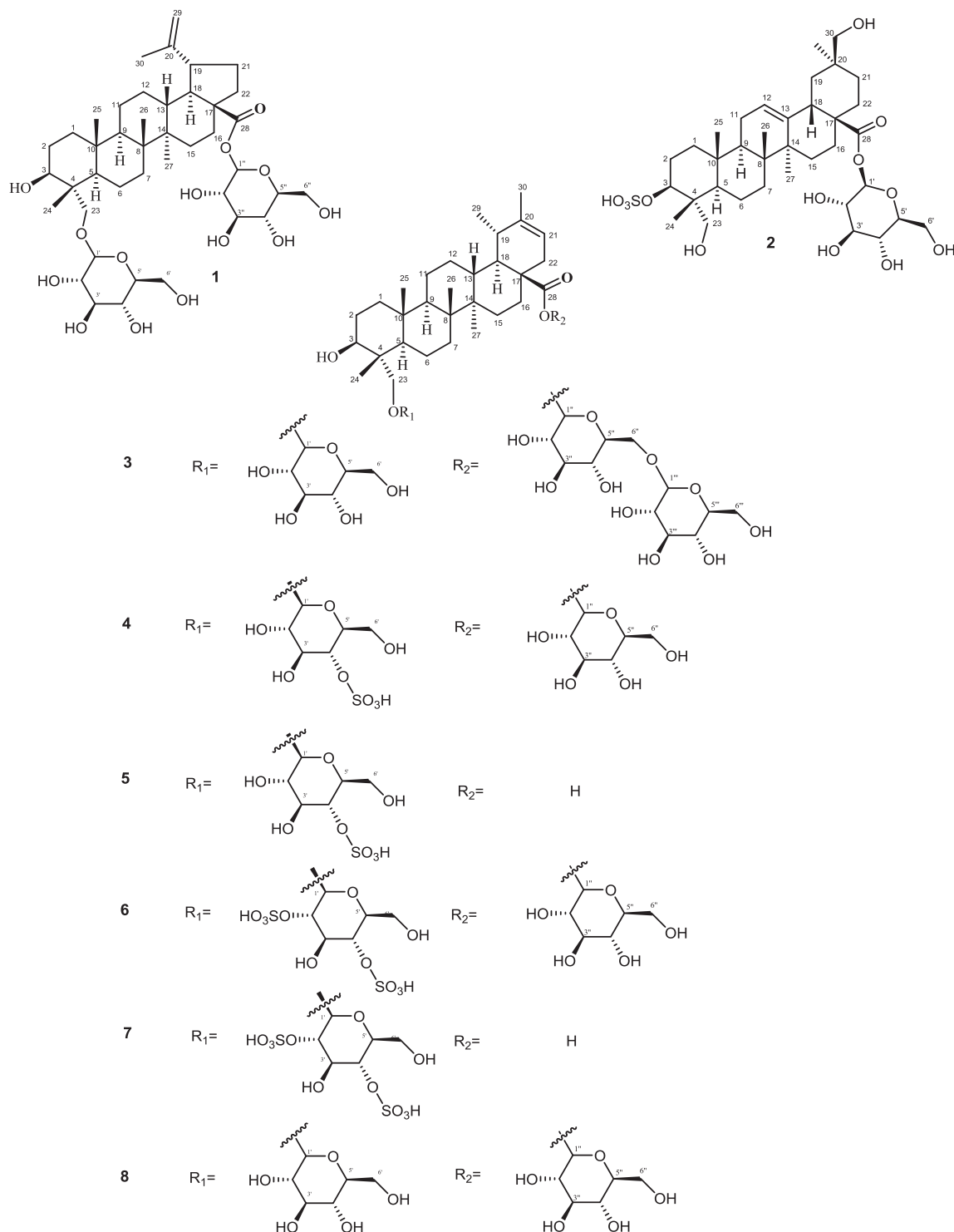


Fig. 1. Structures of compounds **1–8**.

2.1. Identification of the chemical structure of the isolated compounds

Nayabin A (**1**) was obtained as amorphous form, its molecular formula $C_{42}H_{68}O_{14}$, was determined by HR-ESI-MS which showed pseudo-molecular ion peak $[M-H]^-$ ion at m/z 795.4587 (calcd for $C_{42}H_{68}O_{14} - H = 795.4536$), with nine degrees of unsaturation (one $C=O$, one $C=C$, one for each sugar residue, and five remaining to point out all the pentacyclic compounds). Adduct ion $[M+CH_3COOH-H]^-$ at m/z 855.5321 was also observed. MS/MS analysis of compound **1** (negative ion mode), showed the fragment

ion at m/z 633 $[M-H-162]^-$ due to the loss of one glucose moiety.

The 1H and ^{13}C -NMR data (Tables 1 and 2) of compound **1** displayed signals for five tertiary methyls at δ_H 0.67s, 0.86s, 0.94s, 0.97s, and 1.68s; an exo-methylene group at C-29/20 [δ_H 4.70 and 4.58/ δ_C 110.2 (CH_2 -29) and δ_C 151.8 (C-20)]; and an ester carbonyl carbon at δ_C 176.1 (C-28). The 1H and ^{13}C -NMR spectra also showed the signals of two anomeric carbons at δ_H 4.22 (d, $J_{1'/2'} = 8.0$ Hz)/ δ_C 104.7 (C-1') and δ_H 5.47 (d, $J_{1''/2''} = 8.0$ Hz)/ δ_C 95.2 (C-1'') indicating the presence of two sugar moieties in the molecule. In the ^{13}C -NMR spectrum, there is signals for five sp^3 quaternary carbon at δ 43.6 (C-4), 41.9 (C-8), 38.1 (C-10), 43.5 (C-15), 57.9 (C-17). Above

Table 1

1H -NMR spectral data of compounds **1–7**^{a,b}.

No	1	2	3	4	5	6	7
1	1.63, 2.31 m	1.0, 1.62 m	0.91, 1.61 m	0.98, 1.70 m	0.98, 1.70 m	0.98, 1.70 m	1.09, 1.65 m
2	1.00, 1.69 m	1.78, 1.89 m	1.12, 1.71 m	1.61, 1.69 m	1.65, 1.72 m	1.61, 1.69 m	1.61, 1.70 m
3	3.73 ^b	4.25 dd (12.0, 4.5)	4.25 ^b	3.75 ^b	3.74 ^b	3.75 ^b	3.82 d (5.4)
4	—	—	—	—	—	—	—
5	1.21 ^b	1.62 ^b	1.29 ^b	1.22 ^b	1.19 ^b	1.21 ^b	1.19 ^b
6	1.09, 1.52 m	1.45, 1.55 m	1.28, 1.62 m	1.51, 1.72 m	1.49, 1.73 m	1.51, 1.72 m	1.49, 1.74 m
7	1.30, 1.49 m	1.27, 1.49 m	1.31, 1.41 m	1.35, 1.41 m	1.36, 1.43 m	1.35, 1.41 m	1.35, 1.41 m
8	—	—	—	—	—	—	—
9	1.40 m	1.63 m	1.35 m	1.45 m	1.47 m	1.45 m	1.49 m
10	—	—	—	—	—	—	—
11	0.96, 1.42 m	1.70, 2.0 m	1.25, 1.50 m	1.59, 1.62 m	1.59, 1.61 m	1.59, 1.62 m	1.59, 1.62 m
12	1.52, 1.62 m	5.28 t* (3.0)	1.18, 1.71 m	1.63, 1.67 m	1.64, 1.69 m	1.63, 1.67 m	1.63, 1.67 m
13	2.32 m	—	2.64 t d (9.5, 3.5)	2.35 t d (7.5, 3.0)	2.40 t d (7.5, 3.0)	2.35 t d (7.5, 3.0)	2.40 br t (7.5)
14	—	—	—	—	—	—	—
15	1.10, 1.78 m	1.29, 1.46 m	1.12 m, 2.07 br t (13.0)	1.11, 1.59 m	1.11, 1.59 m	1.11, 1.59 m	1.11, 1.59 m
16	1.89, 2.63 m	1.91, 2.10 m	1.42, 2.36 m	1.42, 2.05 m	1.41, 1.92 m	1.42, 2.05 m	1.41, 2.03 m
17	—	—	—	—	—	—	—
18	1.04 ^b	2.80 dd (14.0, 4.0)	1.40 ^b	1.22 ^b	1.22 ^b	1.22 ^b	1.21 ^b
19	2.96 m	1.82, 1.60 m	2.36 m	2.10 m	2.08 m	2.10 m	2.09 m
20	—	—	—	—	—	—	—
21	1.11, 1.21 m	1.24, 1.51 m	5.44 br d (7.0)	5.21 br d (7.0)	5.23 br d (7.0)	5.21 br d (7.0)	5.22 br d (7.0)
22	1.91, 2.01 m	1.23, 1.55 m	1.88 ^b , 2.55 dd (16.0, 7.5)	1.81 br d (15.5), 2.26 dd (15.5, 7.0)	1.78 br d (15.5), 2.20 dd (15.5, 7.0)	1.81 br d (15.5), 2.26 dd (15.5, 7.0)	1.79 br d (15.5), 2.20 dd (15.5, 7.0)
23	3.37, 3.70 ^b	3.30, 3.49 ^b	4.05, 4.18 ^b	3.36, 3.70 ^b	3.36 d (9.5), 3.71 d (9.5)	3.36, 3.70 ^b	3.41 ^b , 3.69 d (10.0)
24	0.67 s	0.68 s	0.96 s	0.68 s	0.68 s	0.68 s	0.69 s
25	0.86 s	0.98 s	0.86 s	0.89 s	0.90 s	0.88 s	0.88 s
26	0.94 s	0.79 s	1.15 s	0.96 s	0.96 s	0.94 s	0.96 s
27	0.97 s	1.18 s	0.88 s	0.99 s	0.99 s	0.98 s	0.99 s
28	—	—	—	—	—	—	—
29	4.70s, 4.58s	0.88s	1.02 d (6.5)	1.01 d (6.5)	1.00 d (6.0)	1.01 d (6.5)	1.01 d (6.5)
30	1.68s	3.41, 3.50 ^b	1.68 s	1.60 s	1.60 s	1.60 s	1.60 s
1'	4.22 d (8.0)	5.35 d (8.0)	4.91 d (8.0)	4.26 d (8.0)	4.27 d (8.0)	4.23 d (8.0)	4.46 d (7.2)
2'	3.26 ^b	3.30 ^b	4.01 ^b	3.29 ^b	3.30 ^b	4.15 t* (9.0)	4.16 t (9.0)
3'	3.27 ^b	3.33 ^b	4.18 ^b	3.64 t (9.0)	3.64 t (9.0)	3.89 ^b	3.88 ^b
4'	3.33 ^b	3.39 ^b	4.24 ^b	4.09 t (9.0)	4.12 t* (9.0)	4.22 t (9.0)	4.23 t* (9.0)
5'	3.39 ^b	3.32 ^b	4.13 ^b	3.39 ^b	3.40 ^b	3.39 ^b	3.42 ^b
6'	3.84 ^b , 3.67 ^b	3.78 br d (10.5), 3.64 br d (11.5, 4.0)	4.38 dd (11.0, 1.5), 4.48 ^b	3.87 dd (12.0, 1.5), 3.67 ^b	3.73 ^b , 3.89 dd (12.0, 1.5)	3.85 dd (11.0, 1.5), 3.67 ^b	3.76 dd (12.6, 7.2), 3.90 br d (12.6)
1''	5.47 d (8.0)	—	6.26 d (8.0)	5.40 d (8.5)	—	5.41 d (8.5)	—
2''	3.2 ^b	—	4.01 ^b	3.26 ^b	—	3.19 t* (8.5)	—
3''	3.38 ^b	—	3.93 ^b	3.38 ^b	—	3.38 ^b	—
4''	3.27 ^b	—	4.20 ^b	3.33 ^b	—	3.27 ^b	—
5''	3.32 ^b	—	4.10 ^b	3.32 ^b	—	3.32 ^b	—
6''	3.81 ^b , 3.64 ^b	—	4.61 dd (11.5, 2.0), 4.26 ^b	3.80 dd (12.0, 2.0), 3.69 ^b	—	3.80 dd (12.0, 2.0), 3.64 ^b	—
1'''	—	—	4.97 d (8.0)	—	—	—	—
2'''	—	—	4.23 ^b	—	—	—	—
3'''	—	—	3.92 ^b	—	—	—	—
4'''	—	—	4.25 ^b	—	—	—	—
5'''	—	—	4.19 ^b	—	—	—	—
6'''	—	—	4.36 ^b , 4.54 dd (11.5, 2.0)	—	—	—	—

t* (footnote: apparent multiplicity = dd).

^a In CD_3OD (δ ppm) for compounds **1–2**, **4–7** and pyridine- d_5 (δ ppm) for **3**; J in Hz.

^b Overlapped signals, reported without assigned multiplicity.

Table 2
¹³C-NMR spectral data of compounds **1–7**^a.

Position	1	2	3	4	5	6	7
1	39.7	39.6	38.9	39.8	39.8	39.5	39.3
2	27.3	24.6	27.8	28.3	28.7	28.7	28.7
3	72.9	80.8	72.1	72.6	72.5	74.2	72.6
4	43.6	43.7	43.0	43.5	43.5	43.5	43.4
5	49.0	48.3	49.2	49.5	49.5	49.8	49.8
6	18.9	19.0	18.5	18.9	18.8	19.0	19.0
7	35.0	33.4	34.3	34.9	35.0	34.8	34.9
8	41.9	40.7	42.3	42.1	41.9	42.1	41.9
9	51.8	49.5	50.9	51.9	51.9	51.5	51.4
10	38.1	37.9	37.2	38.1	38.0	38.0	39.3
11	22.0	24.8	21.9	22.8	22.8	22.8	22.8
12	27.3	124.0	27.7	27.4	27.3	27.4	27.4
13	39.3	144.6	39.5	40.4	40.4	40.5	40.4
14	43.5	43.0	42.3	43.0	43.0	43.1	43.0
15	30.8	28.9	29.5	30.1	30.2	30.2	30.2
16	32.8	24.3	33.4	33.7	34.1	33.7	34.0
17	57.9	47.9	49.7	50.4	49.9	50.4	49.9
18	50.6	42.0	48.7	50.3	50.9	50.3	50.0
19	48.3	42.4	37.6	38.5	38.6	38.5	38.5
20	151.8	46.1	143.1	144.0	144.0	144.1	144.1
21	31.4	29.9	117.5	118.2	118.2	118.1	118.1
22	37.4	32.7	37.7	38.3	39.0	38.3	38.9
23	74.1	65.1	74.9	73.9	73.8	75.0	75.0
24	12.7	13.1	13.1	12.8	12.7	12.7	12.6
25	17.4	16.6	17.0	17.4	17.4	17.3	17.2
26	16.6	17.8	16.4	16.6	16.6	16.6	16.5
27	15.1	26.4	15.2	15.3	15.2	15.5	15.4
28	176.1	178.0	177.5	175.8	180.0	175.9	179.8
29	110.2	28.0	23.6	23.8	23.9	23.8	23.8
30	19.5	66.3	22.2	22.1	22.1	22.1	22.0
1'	104.7	95.7	105.5	104.3	104.3	102.8	102.8
2'	74.1	73.9	75.2	74.2	75.0	81.4	81.0
3'	77.9	78.3	78.7	77.0	76.9	72.7	75.0
4'	71.1	71.1	71.7	78.6	77.8	77.4	77.2
5'	78.4	78.6	78.6	76.3	76.2	76.2	76.1
6'	62.9	62.4	62.9	62.7	62.5	62.6	62.4
1''	95.2		95.2	95.3		95.2	
2''	75.2		75.2	75.2		75.7	
3''	78.3		78.5	78.3		78.3	
4''	71.7		71.5	71.4		71.1	
5''	78.7		78.4	77.9		78.6	
6''	62.5		69.4	62.5		62.5	
1'''			105.3				
2'''			74.3				
3'''			77.9				
4'''			71.1				
5'''			78.8				
6'''			62.7				

^a In CD₃OD (δ ppm) for compounds **1–2**, **4–7** and pyridine-d₅ (δ ppm) for compound **3**; *J* in Hz.

mentioned facts indicated that aglycone part of the compound is lupane class of triterpene similar to bourneioside A, with only the difference of position of glucose moiety on C-23 instead of C-3 (Xiang et al., 2000). The up-field shift of C-1'' (δC 95.2) signal suggested that unit was an ester substituent of C-28 acid function, which was further confirmed by the HMBC correlation between H-1'' (δH 5.47) and C-28 (δC 176.1) (Shaker et al., 1999; Xiang et al., 2000). An HMBC correlation observed between H-1' of glucose moiety (δH 4.22) and the carbon C-23 (δC 74.1) confirmed the position of other glucose. Key HMBC and COSY-45° interactions of compound **1** are presented in Fig. 2. Stereochemistry of compound **1** was assigned on the biogenesis basis and NOESY correlation (Fig. 3). A NOESY correlation signal between the H-5 (δH 1.21), H-3 (δH 3.73) and H-9 (δH 1.40) was consistent with the α-orientation. In addition, the key correlations of Me-24β/Me-25β, Me-25β/Me-26β and Me-26β/H-13β showed that Me-24, Me-25, Me-26, H-13 were on the same face, so the relative stereochemistry were determined. NOESY correlation between H-18 (δH 1.04) and Me-27

(δH 0.97) suggested that the C-27 methyl group possessed α-orientation. The configuration of the sugar unit was assigned as D-glucose as described in section 3.5. Hence, the structure of compound **1** was characterized as β-D-glucopyranosyl 3β-hydroxy-23-β-D-glucopyranosyloxy-lup-20(29)-en-28-oate.

The molecular formula of nayabin B (**2**) was deduced from the ESI-QTOF-MS (negative ion mode), which displayed [M-H]⁻ ions at *m/z* 729.3496 (calcd for C₃₆H₅₈O₁₃S - H = 729.3525), with eight degrees of unsaturation. In the ESI-MS/MS spectra of **2** (negative ion mode), the product ion observed at *m/z* 567 [M-H-162]⁻ suggest the loss of hexose unit. Fragment ion at *m/z* 303 [M-H-162-264]⁻ was supposed to be generated from *m/z* 567 by retro Diels-Alder cleavage of ring C. Another product ion at *m/z* 97 was indicating the fragment of sulfate group [HSO₄]⁻ (Perrone et al., 2007; Shaker et al., 2000).

The ¹H-NMR spectrum (Table 1) of **2** displayed five singlets for tertiary methyls at δH 0.68, 0.98, 0.79, 1.18 and 0.88 assigned to Me-24, Me-25, Me-26, Me-27 and Me-29, respectively. Furthermore, in ¹H and ¹³C-NMR spectra, signals for one olefinic methine at δH/δC 5.28 (t, *J*_{12/11} = 3.0 Hz)/124.0 (C-12), carboxyl ester at δC 178.0 (C-28) and two hydroxymethylenes at δH/δC 3.30, 3.49/δC 65.1 (C-23) and 3.41, 3.50/66.3 (C-30) were observed. An oxygenated methine signal at δH/δC 4.25 (dd, *J*_{3/2ax} = 12.0 Hz, *J*_{3/2eq} = 4.5 Hz)/80.8 was assigned to CH-3. The ¹³C-NMR spectrum displayed resonances for six sp³ quaternary carbons at δC 43.7 (C-4), 40.7 (C-8), 37.9 (C-10), 43.0 (C-14), 47.9 (C-17), and 46.1 (C-20). Anomeric carbon signals were observed at δH/δC 5.35 (d, *J*_{1'/2'} = 8.0 Hz)/95.7 (C-1'). Above discussed fact clearly indicated that aglycone part of the compound **2** is oleanane type tri-terpene (Khalik et al., 2000; Luo et al., 2011; Miyakoshi et al., 1997). The downfield shift of H-3 indicated the substitution of sulfate group on hydroxyl group (Perrone et al., 2007). In HMBC spectrum (Fig. 2), anomeric proton at δH 5.35 showed correlation with C-28, which indicated the position of sugar moiety. Stereochemistry at C-3 was assigned on the basis of coupling constants values of H-3, which showed *J* = 12.0, and 4.5 Hz. It indicated that H-3 position is axially oriented, which was further supported by a NOESY cross-peak between H-5 (δH 1.62) and H-3 (δH 4.25) (Fig. 3). The stereochemistry at C-20 was assigned based on carbon value of C-20, as reported in literature (Luo et al., 2011; Miyakoshi et al., 1997) and also confirmed by NOESY correlation between H-18 and H-30. The stereochemistry of the several centers was demonstrated by NOESY spectrum showing connectivities between Me-24β/Me-25β, Me-25β/Me-26β, H-3α/H₂-23 and H-5α/H-9α. The configuration of the sugar unit was assigned as D-glucose. Thus, the structure of **2** was identified as β-D-glucopyranosyl 3β-O-sulfo-23,30-dihydroxy-olean-12-en-28-oate.

The ESI-QTOF-MS (negative ion mode) of nayabin C (**3**) showed a peak at *m/z* 957.5020 (calcd. for C₄₈H₇₈O₁₉ - H = 957.5064), ten degrees of unsaturation. In the ESI-MS/MS spectra of **3** (negative ion mode), the fragment ion observed at *m/z* 633 [M-H-324]⁻ suggests the loss of two glucose moieties.

The ¹H-NMR of the aglycone part displayed five tertiary methyl protons at δH 0.96, 0.86, 1.15, 0.88, 1.68, (each s) and 1.02 d (*J*_{29/18} = 6.5 Hz). ¹H and ¹³C-NMR (Tables 1 and 2) spectra of **3** showed signals at [δH 4.25 (overlap)/δC 72.1; CH-3], [δH 5.44 (br d, *J*_{21/22} = 7 Hz)/δC 117; CH-21], C-23 hydroxymethyl group [δH 4.05 and 4.18 (each overlap)/δC 74.9; CH₂-23] and at δC 143.1 (C-20), δC 177.5 (C-28). The ¹³C-NMR spectrum displayed resonances for five sp³ quaternary carbons at δC 43.0 (C-4), 42.3 (C-8), 37.2 (C-10), 42.3 (C-14), and 49.7 (C-17). The ¹H- and ¹³C-NMR spectra showed the presence of three anomeric signals at δH/δC 4.91 (d, *J*_{1'/2'} = 8.0 Hz)/105.5; δH/δC 6.26 (d, *J*_{1'/2'} = 8.0 Hz)/95.2 and δH/δC 4.97 (d, *J*_{1'''/2'''} = 8.0 Hz)/105.3 indicated the presence of three hexose units. Above mentioned data indicated that aglycone part of **3** was similar to taraxastane type triterpene reported in literature (Ansari et al.,

1987). The up-field shift of one glucose anomeric carbon C-1'' (95.2) signal suggested the unit was an ester substituent of C-28 acid function. The (1 → 6) linkage between terminal β -D-glucopyranosyl residue and the other terminal β -D-glucopyranosyl unit was confirmed by HMBC correlations observed between C-6'' at δ 69.4 and C-1''' at δ 4.97. The position of third sugar was assigned on the basis of HMBC correlations between H-1' (δ_H 4.91) and C-23. In the HMBC spectrum, the methyl signal at δ_H 1.68 (H-30) showed long-range correlations with olefinic carbon signals at δ_C 117.5 and δ_C 143.1, which hinted the position of olefinic carbon in the compound. Key HMBC and COSY-45° interactions of compound **3** are presented in Fig. 2. In NOESY spectrum (Fig. 3), the key correlations of Me-24 β /Me-25 β , Me-25 β /Me-26 β , H₂-23/H-5 α and H-18 α /Me-27 α showed that Me-24, Me-25, Me-26 were on the same face, so the relative stereochemistry were determined. The configuration of sugar was assigned as β on the basis of coupling constant values of anomeric protons (Khalik et al., 2000). The sugars were identified as D-glucose. Thus, the structure of **3** was established β -D-glucopyranosyl-(1 → 6)- β -D-glucopyranosyl 3 β -hydroxy-23- β -D-glucopyranosyloxy-taraxast-20-en-28-oate.

Nayabin D (**4**) in negative ESI-QTOF-MS showed a [M-H]⁻ at m/z 875.4140, ascribable to the molecular formula C₄₂H₆₇O₁₇S (calcd for C₄₂H₆₈O₁₇S - H = 875.4104). In the ESI-MS/MS spectra of **4** (negative ion mode), the product ions observed at m/z 713 [M-H-162]⁻ and m/z 471 [M-H-162-242]⁻ suggest the loss of hexose sugar and sulfate-hexose unit, respectively. Other product ions at m/z 97 and m/z 241 indicated the characteristic fragment of sulfate group [HSO₄]⁻ and sulfate-hexose unit [C₆H₉O₈S]⁻, respectively (Perrone et al., 2007; Shaker et al., 2000).

The ¹H- and ¹³C- NMR spectra showed signals of two anomeric carbons at δ_H/δ_C 4.26 (d, $J_{1'2'} = 8$ Hz)/104.3 and 5.40 (d, $J_{1'2'} = 8.5$ Hz)/95.2. Structure of compound **4** was found to be similar to compound **3**, with only the differences of absence of one sugar unit and the presence of sulfate group on C-4'. The downfield shift of H-4' (δ_H 4.09, t, $J_{4,3/4,5} = 9.0$ Hz) and C-4' (δ_C 78.6) also indicated the substitution of sulfate group on the OH group of C-4' sugar moiety (Perrone et al., 2007; Shaker et al., 2000). This was further confirmed from COSY and HMBC spectra. In COSY spectrum, H-4' (δ_H 4.09) showed correlations with H-3' (δ_H 3.64) and H-5' (δ_H 3.39), furthermore H-3' showed correlation with H-2' (δ_H 3.29), which is correlated to the anomeric proton H-1' (δ_H 4.26). In HMBC spectrum, H-4' (δ_H 4.09) showed correlations with C-3' (δ 77.0), C-5' (δ 76.3), and C-6' (δ 62.7), which further supported the position of sulfate group. Stereochemistry of compound **4** was similar to compound **3**. Hence, the structure of **4** was identified as the β -D-glucopyranosyl 3 β -hydroxy-23-(4'-O-sulfo- β -D-glucopyranosyloxy)-taraxast-20-en-28-oate.

Nayabin E (**5**) in negative ESI-QTOF-MS showed a [M-H]⁻ at m/z 713.3541 (calcd for C₃₆H₅₈O₁₂S - H = 713.3576). In the ESI-MS/MS spectra of **5** (negative ion mode), the product ions observed at m/z 97 and m/z 241 indicated the characteristic fragments of sulfate group [HSO₄]⁻ and sulfate-hexose unit [C₆H₉O₈S]⁻, respectively (Perrone et al., 2007; Shaker et al., 2000).

The ¹H and ¹³C-NMR spectrum (Tables 1 and 2) showed signal of an anomeric methine at δ_H/δ_C 4.27 (d, $J_{1'2'} = 8.0$ Hz)/104.3, which inferred that there is a sugar moiety in the molecule. Connectivity of sugar moiety with C-23, was confirmed by the HMBC correlation between H-1' (δ_H 4.26) and C-23 (δ_C 73.8). Comparison of NMR data of **4** and **5** indicated structural similarities, with only the difference that compound **5** is the corresponding free acid of compound **4**. Hence, the structure of **5** was identified as the 3 β -hydroxy-23-(4'-O-sulfo- β -D-glucopyranosyloxy)-taraxast-20-en-28-oic acid.

Compound **6** in negative ESI-QTOF-MS showed a [M-H]⁻ at m/z 955.3645 (calcd for C₄₂H₆₈O₂₀S₂ - H = 955.3672). The ESI-MS/MS showed a prominent fragment ion peak at m/z 875 [M-H-

162]⁻ due to loss of one hexose unit. Other fragment ions observed at m/z 321, 241 and 97 indicated the characteristic fragments of disulfate-hexose unit [C₆H₉O₁₁S₂]⁻, sulfate-hexose unit [C₆H₉O₈S]⁻, and sulfate group [HSO₄]⁻, respectively (Perrone et al., 2007; Shaker et al., 2000).

Analysis of the ¹H and ¹³C-NMR data (Tables 1 and 2) of **6** inferred that the compound was similar to the compound **4**, the only difference being the presence of two sulfate group in **6** instead of one in compound **4**. The downfield shift of protons H-2' (δ_H 4.15, dd, $J_{2,1/2,3} = 9.0$ Hz) and H-4' (δ_H 4.22, t, $J_{4,3/4,5} = 9.0$ Hz) indicated the substitution of sulfate group on the OH groups of C-2' and C-4' of glucose unit. This was further confirmed by COSY and HMBC spectra. In COSY-45° spectrum, H-2' (δ_H 4.15) showed correlations with H-1' (δ_H 4.23) and H-3' (δ_H 3.89), furthermore H-3' showed correlations with H-4' (δ_H 4.22). In HMBC spectrum, H-2' showed correlation with anomeric carbon (C-1'), and H-4' showed correlations with C-5' and C-6', which clearly indicated the position of sulfate groups. Accordingly, the structure of **6** was assigned as β -D-glucopyranosyl 3 β -hydroxy-23-(2',4'-di-O-sulfo- β -D-glucopyranosyloxy)-taraxast-20-en-28-oate.

Compound **7** in negative ESI-QTOF-MS showed a [M-H]⁻ at m/z 793.3160 (calcd for C₃₆H₅₈O₁₅S₂ - H = 793.3144). MS/MS analysis of compound **7** showed the characteristic fragment ions at m/z 321, 241 and 97, due to the presence of sulfate group like in compounds **2**, **4**, **5** and **6**. Comparison of ¹H and ¹³C-NMR data (Tables 1 and 2) of Nayabin G (**7**) with Nayabin F (**6**) indicated structural similarities, except for a free C-28 carboxyl in **7**. Analysis of ¹H and ¹³C-NMR spectrum showed signal of only one anomeric carbon at δ_H/δ_C 4.46 (d, $J_{1'2'} = 7.2$ Hz)/102.8. Hence, the structure of **7** was identified as the 3 β -hydroxy-23-(2',4'-di-O-sulfo- β -D-glucopyranosyloxy)-taraxast-20-en-28-oic acid.

The known compound **8** (Ansari et al., 1987; Farheen et al., 2015) was obtained as amorphous form with the molecular formula C₄₂H₆₈O₁₄, as determined by the data of positive ion high resolution electrospray ionization mass spectrum (HR-ESI-MS) showing an [M+H]⁺ ion at m/z 797.4698 (calcd for C₄₂H₆₈O₁₄ + H = 797.4681). Deduced molecular formula of compound **8** was lower by C₆H₁₀O₅ than that of compound **3**. ¹H and ¹³C NMR values and spectra are given in Table S1 in supplementary data.

2.2. Insulin secretory activity

To elucidate the importance of these isolated compounds, we have performed a series of bioassays; however, insulin secretory activity was found promising in our *in-vitro* insulin secretory assay system. These compounds were explored further to identify novel insulin secretagogues that stimulate insulin secretion at stimulatory glucose concentrations rather than basal glucose concentrations that may serve as better insulin secretagogues compared with standard sulfonylurea drugs. In our assay, compounds **1**, **3**, **4**, **5** and **8** were screened to check their potential against insulin secretory activity and compared with tolbutamide, a known insulin secretagogue. Compounds **1**, **3**, **4**, and **5** showed little to no insulin secretory activity both at basal and high glucose concentrations (data not shown). Interestingly, compound **8** showed potent insulin secretory activity at high glucose concentration, but not at basal glucose concentration. Due to limited amount, other compounds could not be tested for their bioactivities.

2.2.1. Glucose-dependent insulin secretory activity of compound **8** in isolated mice islets

The effects of compound **8** on glucose-stimulated insulin secretion from mice islets are compared with tolbutamide and summarized in Fig. 4. At basal (3 mM) glucose concentration, compound **8** of doses 0.1–200 μ M has no effect on insulin secretion

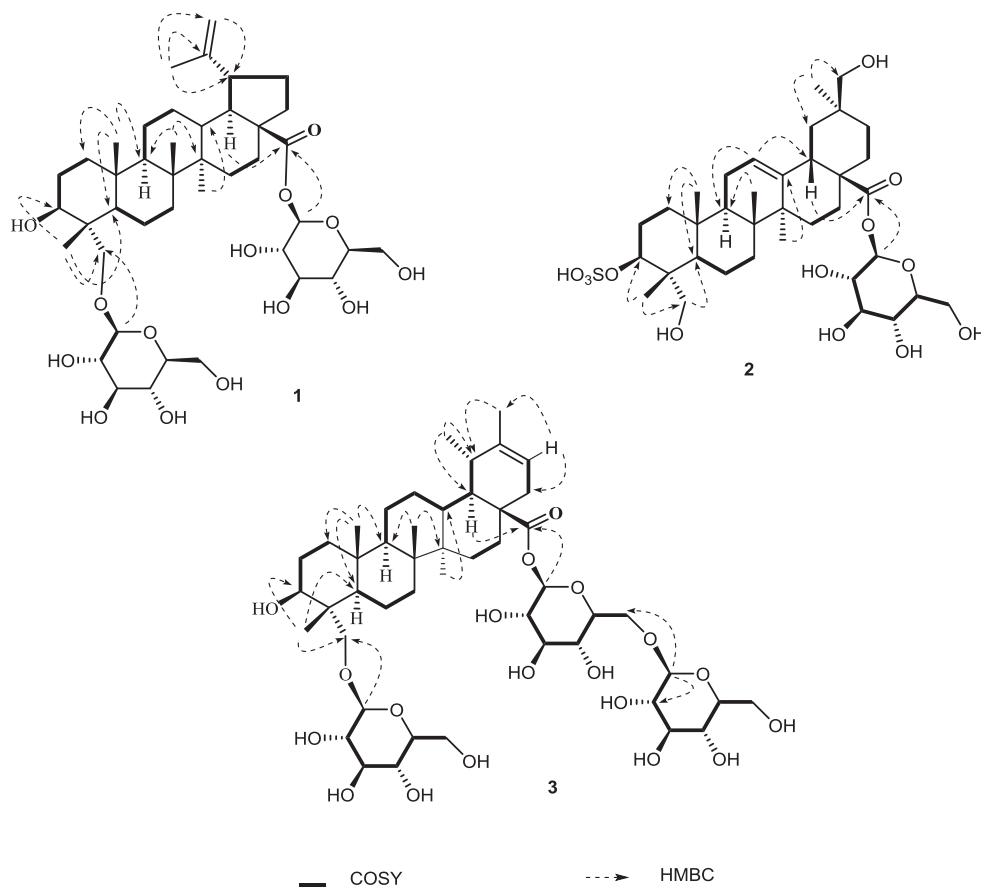


Fig. 2. Key HMBC and COSY-45° interactions of compounds **1**, **2**, and **3**.

(Fig. 4A). In contrast to compound **8**, tolbutamide showed potent insulinotropic effect at basal glucose. Interestingly, compound **8** enhanced insulin secretion at stimulatory (16.7 mM) glucose concentration. At 0.1 μM dose, compound **8** showed little to no effect on insulin secretion. At 1 μM dose, compound **8** showed significant

($P < 0.05$) effect on stimulation of insulin secretion ($387.1 \pm 22.1\%$) compared to control ($320.9 \pm 9.2\%$). The dose 10 μM showed maximum ($P < 0.01$) increase in insulin secretion ($511.4 \pm 32.7\%$) that is comparable with insulin secretory effect of tolbutamide ($622.4 \pm 35.7\%$). Increasing the dose of compound **8** above 10 μM ,

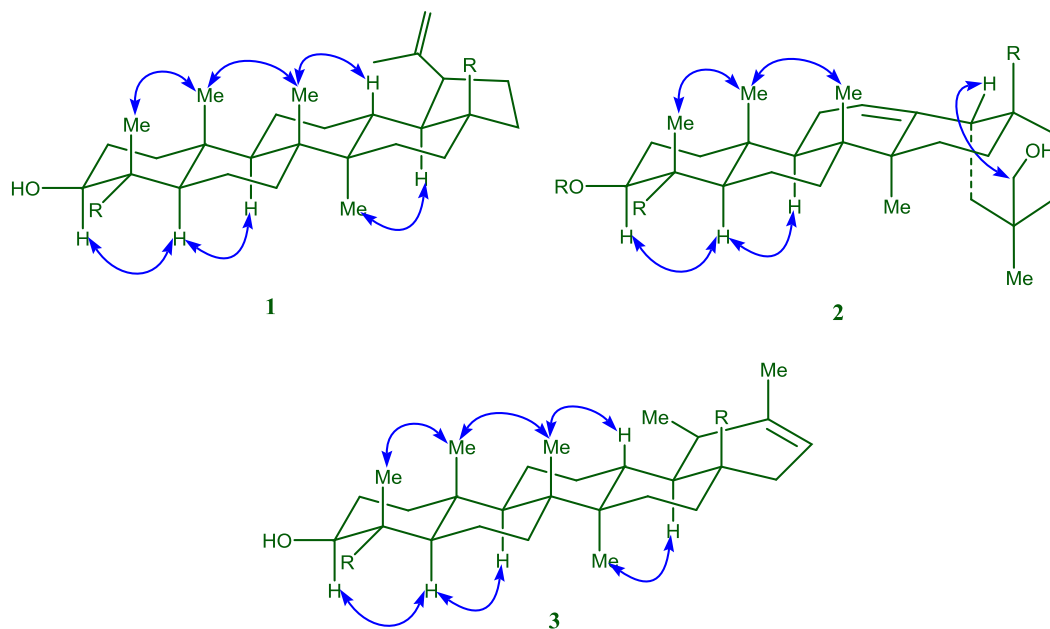


Fig. 3. Key NOESY interactions of compounds **1**, **2**, and **3**.

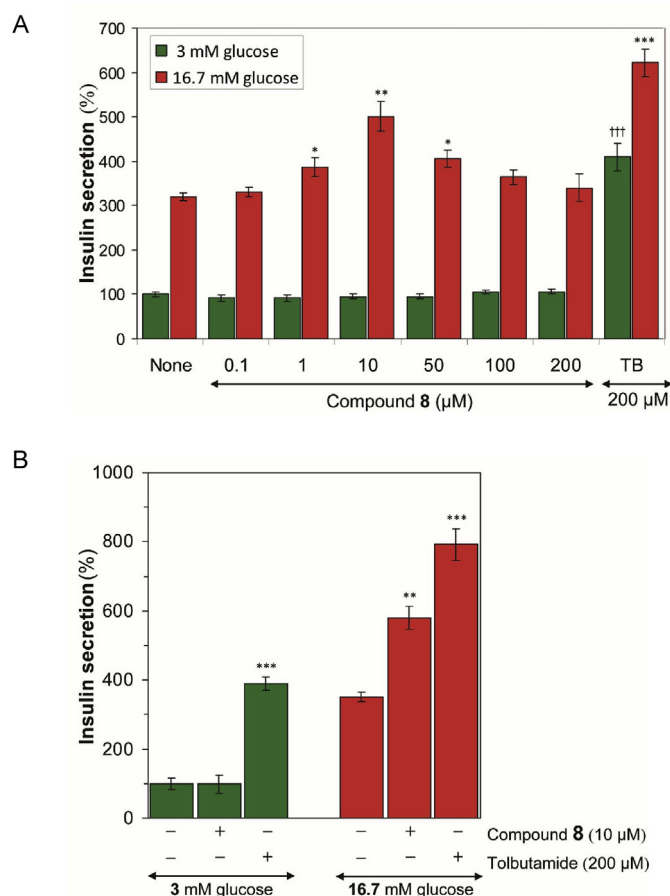


Fig. 4. Concentration- and glucose-dependent modulation of insulin secretion in mice islets by compound **8**. Islets were incubated for 1 h at 37 °C in KRB buffer containing 3 mM and 16.7 mM glucose in the absence or presence of test compound and secreted insulin was measured. (A) Islets were incubated in KRB buffer containing 3 mM and 16.7 mM glucose with different concentrations of compound **8**; TB, insulin secretion by tolbutamide. (B) Islets were incubated in KRB buffer containing 3 mM and 16.7 mM glucose in the absence or presence of either compound **8** or tolbutamide at indicated concentrations. Percentage relative insulin secretions were calculated and insulin secretion activities by 3 mM glucose were taken as 100%. All data points are an average of a minimum of $n = 4$ separate experiments and are expressed as means \pm SEM. * $P < 0.05$, ** $P < 0.01$, *** $P < 0.001$, symbolizes a significant difference (t -test) in insulin secretion over the respective control values.

no further improvement of insulin secretion was observed. These data suggest that compound **8** works at stimulatory glucose only in a narrow range of concentrations and below and above the window it is not active.

Furthermore, we evaluated the glucose-dependent and/or K-ATP channels-dependent behavior of compound **8** by comparing with tolbutamide, a standard insulin secretagogue (Fig. 4B). It is reported that tolbutamide enhanced insulin secretion by blocking K-ATP channels and stimulates insulin secretion in depolarization-dependent mechanism irrespective of glucose concentrations. We also found that tolbutamide significantly stimulated insulin secretion both at basal and stimulatory glucose concentrations (Fig. 4B), and the insulin stimulation was higher at basal glucose (4-fold) than that of stimulatory glucose (2.2-fold) concentration. To the contrary, compound **8** showed insulin secretory activity only at stimulatory glucose, distinctly different from that of tolbutamide. Compound **8** enhances glucose-stimulated insulin secretion and most importantly it works at low concentration (10 μM) per se better than standard drug tolbutamide. These data suggest that the mode of action of compound **8** is different from tolbutamide.

It has been reported that a few novel imidazoline compounds

(e.g. BL11282) potentiate glucose-induced insulin secretion in pancreatic β -cells in the absence of modulation of K-ATP channels (Efanov et al., 2001). Few non-imidazoline compounds also showed glucose-dependent insulinotropic effects. Genistein, a flavanoid, did not affect insulin release at non-stimulatory concentrations of glucose; however, at the stimulatory concentrations of glucose, genistein significantly increased insulin secretion in a dose-dependent manner (Liu et al., 2006; Ohno et al., 1993). Resveratrol, a polyphenol, potentiates insulin secretion exclusively in a glucose-dependent manner in INS-1E β -cells (Vetterli et al., 2011). Recently, we have also reported that bergenicin from *Bergenia himalaica* showed glucose-dependent insulinotropic effects in isolated mice islets (Siddiqui et al., 2014). Furthermore, the glucose concentration-dependent insulinotropic activity of compound **8** suggests possible low risk of hypoglycemia and may offer distinct advantages as anti-diabetic agent that may further proceed as a drug candidate. Further study(ies) is(are) needed to elucidate the exact mechanism(s) of compound **8** mediated insulin secretion. Compound **8** was evaluated for its cytotoxicity in MIN6 cells using 3-[4,5-dimethylthiazole-2-yl]-2,5-diphenyl-tetrazolium bromide (MTT) assay as described previously (Hafizur et al., 2015; Sharma et al., 2015). No significant toxic effect was found up to 200 μM of compound **8**, such nontoxic property may assure its safe use for further investigations.

3. Experimental section

3.1. General experimental procedure

Optical rotations were measured on JASCO P-2000 polarimeter. Infrared (IR) spectra were recorded on a Bruker vector-22 (Germany). ID- and 2D- NMR spectra (^1H , ^{13}C , HSQC, HMBC, COSY, and NOESY) were performed using Bruker Avance-NMR (500 and 600 MHz) spectrometers. All compounds were recorded in solvent CD_3OD except compound **3** which was recorded in pyridine- d_5 . Multiplicities of carbon signals were determined using DEPT 90° and 135°. COSY-45° experiment was used to determine homonuclear ^1H – ^1H correlation. Heteronuclear one-bond ^1H – ^{13}C scalar coupling were studied through HSQC experiment. Multiple bonds heteronuclear ^1H – ^{13}C correlations were studied through HMBC experiment. ESI-QTOF-MS and ESI-QTOF-MS/MS (positive and negative mode) analysis were recorded on QSTAR XL mass spectrometer (Applied Biosystems, USA). The samples were introduced by direct infusion in a solution of MeOH at a rate of $5 \mu\text{M min}^{-1}$. TLC was carried out on reversed phase silica gel RP-18 F254s (Merck) with different composition of MeOH– H_2O mixture. Ceric sulfate was used for visualizing compounds on TLC. Isolation was carried out through column chromatography and recycling preparative HPLC. Column chromatography was utilized for fractionation using silica gel (63–200 μm, Merck) and POLYGOPREP 100-30 C18 (25–40 μm, Macherey Nagel). Recycling preparative HPLC-LC-908, equipped with JAIGEL-ODS-L-80 (L = 250 mm, I.D. = T20 mm), was used to purify compounds.

3.2. Plant material

Whole plant of *Fagonia indica* Burm (Zygophyllaceae) was collected from superhighway, Karachi, Pakistan in 2013. Plant material was identified at the Department of Botany, University of Karachi, Karachi, Pakistan. The voucher specimen (93140) was deposited at the Herbarium, University of Karachi.

3.3. Extraction and isolation

Dried powdered of whole plant of *Fagonia indica* (7.5 kg) was

extracted with 80% methanol. After removal of solvent through evaporation, the resulting residue was fractionated with hexanes, EtOAc, and n-BuOH, subsequently using H₂O. The n-BuOH fraction (500 g) was subjected to vacuum liquid chromatography on reversed phase silica gel RP-18 (10% MeOH to 100% MeOH, gradually increased by 10). As a result, ten fractions F1–F10 were obtained. Fraction 1 was subjected to CC silica gel using ethyl acetate and MeOH to afford fifteen fractions (B1–B15). Further purification of fraction B5 was carried out by reversed phase column chromatography using MeOH and H₂O and finally by reversed phase recycling HPLC (MeOH–H₂O, 50/50), to give compound **2**. Fraction 7 was direct subjected to recycling HPLC (MeOH–H₂O, 70/30), to give compounds **1**, **3**, **4**, **6–8**. Fraction 8 was also direct subjected to reversed phase recycling HPLC (MeOH–H₂O, 70/30), to give compound **5**.

3.4. Compounds characterization

3.4.1. Nayabin A (**1**)

White amorphous powder; Yield: 5.3 mg; $[\alpha]_D^{25} + 35.8$ ($c = 0.28$, MeOH); ¹H-NMR (CD₃OD, 500 MHz) and ¹³C-NMR (CD₃OD, 125 MHz): (See Tables 1 and 2). HRESI-MS m/z 795.4587 [M – H][–] (mol. formula, C₄₂H₆₇O₁₄, calcd. for 795.4536); ESI-MS/MS: m/z 633 [M–H–162][–]; IR (KBr) ν_{\max} cm^{–1}: 3428, 2928, 1738, 1076.

3.4.2. Nayabin B (**2**)

Yellowish white amorphous; Yield: 2.9 mg; $[\alpha]_D^{25} + 25.2$ ($c = 0.17$, MeOH); ¹H-NMR (CD₃OD, 500 MHz) and ¹³C-NMR (CD₃OD, 125 MHz): (See Tables 1 and 2). HR-ESI-MS (negative mode): m/z 729.3496 [M – H][–] (Mol. formula, C₃₆H₅₇O₁₃S, calcd. for 729.3525). ESI-MS/MS: m/z 567 [M–H–162][–]; m/z 303 [M–H–162–264][–]; m/z 97 [HSO₄][–]; IR (KBr) ν_{\max} cm^{–1}: 3428, 2947, 1730, 1208, 985.

3.4.3. Nayabin C (**3**)

White amorphous powder; Yield: 5.9 mg; $[\alpha]_D^{25} + 18$ ($c = 0.2$, MeOH); ¹H-NMR (C₅D₅N, 500 MHz) and ¹³C-NMR (C₅D₅N, 125 MHz): (See Tables 1 and 2). HR-ESI-MS m/z 957.5020 [M – H][–] (mol. formula, C₄₈H₇₇O₁₉, calcd. for 957.5064); ESI-MS/MS: m/z 633 [M–H–162–162][–]; IR (KBr) ν_{\max} cm^{–1}: 3418, 2939, 1736, 1075.

3.4.4. Nayabin D (**4**)

White crystalline solid; Yield: 6.8 mg; $[\alpha]_D^{25} + 44.7$ ($c = 0.27$, MeOH); ¹H-NMR (CD₃OD, 500 MHz) and ¹³C-NMR (CD₃OD, 125 MHz): (See Tables 1 and 2). HR-ESI-MS m/z 875.4140 [M – H][–] (mol. formula, C₄₂H₆₇O₁₇S, calcd. for 875.4104); ESI-MS/MS: m/z 713 [M–H–162][–]; m/z 471 [M–H–162–242][–]; m/z 241 [M–H–162–472][–]; m/z 97 [M–H–162–616][–]; IR (KBr) ν_{\max} cm^{–1}: 3428, 2928, 1736, 1206, 1074, 978.

3.4.5. Nayabin E (**5**)

White amorphous powder; 4.6 mg; $[\alpha]_D^{25} + 58$ ($c = 0.24$, MeOH); ¹H-NMR (CD₃OD, 600 MHz) and ¹³C-NMR (CD₃OD, 150 MHz): (See Tables 1 and 2). HRESI-MS m/z 713.3541 [M – H][–] (mol. formula, C₃₆H₅₇O₁₂S, calcd. for 713.3576); ESI-MS/MS: m/z 471 [M–H–242][–]; m/z 241 [M–H–472][–]; m/z 97 [M–H–616][–]; IR (KBr) ν_{\max} cm^{–1}: 3425, 2929, 1723, 1211, 1072, 981.

3.4.6. Nayabin F (**6**)

Yellowish white solid; Yield: 3.0 mg; $[\alpha]_D^{25} + 53$ ($c = 0.19$, MeOH); ¹H-NMR (CD₃OD, 600 MHz) and ¹³C-NMR (CD₃OD, 150 MHz): (See Tables 1 and 2). HRESI-MS m/z 955.3645 [M – H][–] (mol. formula, C₄₂H₆₇O₂₀S₂, calcd. for 955.3672); ESI-MS/MS: m/z 875 [M–H–162][–]; m/z 321 [M–H–162–342][–]; m/z 241 [M–H–162–472][–]; m/z 97 [M–H–162–616][–]; IR (KBr) ν_{\max} cm^{–1}: 3420, 2940,

1739, 1207, 1071, 978.

3.4.7. Nayabin G (**7**)

White amorphous powder; 3.1 mg; $[\alpha]_D^{25} + 64$ ($c = 0.20$, MeOH); ¹H-NMR (CD₃OD, 600 MHz) and ¹³C-NMR (CD₃OD, 150 MHz): (See Tables 1 and 2). HR-ESI-MS m/z 793.3160 [M – H][–] (mol. formula, C₃₆H₅₇O₁₅S₂, calcd. for 793.3144); ESI-MS/MS: m/z 321 [M–H–472][–]; m/z 241 [M–H–552][–]; m/z 97 [M–H–696][–]; IR (KBr) ν_{\max} cm^{–1}: 3421, 2936, 1720, 1217, 1071, 978.

3.4.8. β -D-Glucopyranosyl 3 β -hydroxy-23-O- β -D-glucopyranosyloxy-taraxast-20-en-28-oate (**8**)

White amorphous powder; Yield: 18.2 mg; $[\alpha]_D^{25}$ Observed: +10 ($c = 0.34$, MeOH); ¹H-NMR (CD₃OD, 500 MHz) and ¹³C-NMR (CD₃OD, 125 MHz): (See Table S1). HRESI-MS m/z 797.4698 [M + H]⁺ (mol. formula, C₄₂H₆₉O₁₄, calcd. for 797.4681); ESI-MS/MS: m/z 633 [M–H–162][–]; IR (KBr) ν_{\max} cm^{–1}: 3418, 2927, 1735, 1076.

3.5. Acid hydrolysis and GC analysis

Each saponin (2 mg) was refluxed with HCl (0.5 N, 2 mL) for 2 h. The hydrolyzed product was extracted with CH₂Cl₂. The residue obtained on usual workup of the aqueous layer was derivatized by adding 100 μ L methoxylamine hydrochloride in pyridine (20 mg mL^{–1}), vortexed and incubated at 60 °C for 45 min. Then 200 μ L of *N,O*-Bis(trimethylsilyl)trifluoroacetamide (BSTFA) was added and incubated at 60 °C for 45 min. The derivatized sample was centrifuged at 6000 rpm for 5 min at 25 °C to remove any solid debris. GC-MS analysis was performed using 7890A gas chromatograph (Agilent technologies, USA), equipped with an Agilent Technology GC autosampler 120 (PAL LHX-AG12) and coupled to an Agilent 7000 Triple Quad system (Agilent technologies, USA). HP-5MS 30m–250 mm (i.d.) fused-silica capillary column (Agilent J & W Scientific, Folsom, CA, USA), chemically bonded with a 5% diphenyl 95% dimethylpolysiloxane cross-linked stationary phase (0.25 mm film thickness) was used. Separation was achieved with a temperature program of 80 °C for 2 min, then ramped at 5 °C min^{–1} to 300 °C and held for 1 min, and a constant flow of 1.0 mL min^{–1}. MS interface and ion source were set at 280. The configuration was determined by comparing the retention time with derivatives prepared in a similar manner from standard sugar (*t*_R D-glucose 26.6 min).

3.6. Islets isolation and insulin secretory biological assay

Islets were isolated by collagenase digestion from pancreas of BALB/c mice (30–40 g) as described previously (Hafizur et al., 2015; Sharma et al., 2015; Siddiqui et al., 2014). In brief, mice were anaesthetized with sodium thiopental (30 mg/kg) and the pancreas was distended with collagenase solution *via* the common bile duct. Then the whole pancreas was removed and digested at 37 °C in collagenase solution for 15 min. Following purification, islets were manually hand-picked under a NIKON SMZ-745 stereomicroscope. The isolation and purification medium used was Hank's Balanced Salt Solution (HBSS) without calcium, magnesium and phenol red. After isolation, batches of three size-matched islets were incubated for 60 min in KRB buffer containing 3 mM (basal) and 16.7 mM (stimulatory) glucose in the presence or absence of test compound. After incubation periods, 100 μ L supernatant was collected and secreted insulin was measured using mouse insulin ELISA kit (Crystal Chem Inc., IL, USA).

Acknowledgments

This work was partially supported by a NRPUR Research Grant (20-4091/NRPUR/R&D/HEC/14/375) to M. Hafizur Rahman from Higher Education Commission (HEC), Pakistan. Nayab kanwal is grateful to the HEC for financial support in Ph.D. program.

Appendix A. Supplementary data

Supplementary data related to this article can be found at <http://dx.doi.org/10.1016/j.phytochem.2017.08.005>.

References

- Abdel-Khalik, S., Miyase, T., Melek, F., El-Ashaal, H., 2001. Further saponins from *Fagonia cretica*. *Die Pharm.* 56, 247–250.
- Abirami, V., Khosa, R., Dhar, S., Sahai, M., 1996. Investigation on *Fagonia cretica*—its effect on hormonal profile and immunomodulation in rats. *Anc. Sci. Life* 15, 259–263.
- Ali, S.S., Kasoju, N., Luthra, A., Singh, A., Sharanabasava, H., Sahu, A., Bora, U., 2008. Indian medicinal herbs as sources of antioxidants. *Food Res. Int.* 41, 1–15.
- Amini, E., Nabiuni, M., Baharara, J., Pariwar, K., Asili, J., 2014. Hemolytic and cytotoxic effects of saponin like compounds isolated from Persian Gulf brittle star (*Ophiocoma erinaceus*). *J. Coast. Life Med.* 2, 762–768.
- Ansari, A.A., Kenne, L., Atta-ur-Rahman, 1987. Isolation and characterization of two saponins from *Fagonia indica*. *Phytochemistry* 26, 1487–1490.
- Efanov, A., Zaitsev, S., Mest, H., Raap, A., Appelskog, I., Larsson, O., Berggren, P., Efendic, S., 2001. The novel imidazoline compound BL11282 potentiates glucose-induced insulin secretion in pancreatic β -cells in the absence of modulation of K-ATP channel activity. *Diabetes* 50, 797–802.
- El-Wakil, E.A., 2007. Phytochemical and molluscicidal investigations of *Fagonia arabica*. *Z. Naturforsch. C* 62, 661–667.
- Farheen, R., Siddiqui, B.S., Mahmood, I., Simjee, S.U., Majeed, S., 2015. Triterpenoids and triterpenoid saponins from the aerial parts of *Fagonia indica* Burm. *Phytochem. Lett.* 13, 256–261.
- Hafizur, R.M., Hameed, A., Shukrana, M., Raza, S.A., Chishti, S., Kabir, N., Siddiqui, R.A., 2015. Cinnamic acid exerts anti-diabetic activity by improving glucose tolerance in vivo and by stimulating insulin secretion *in-vitro*. *Phyto-medicine* 22, 297–300.
- Hamliche, V., Maiza, K., 2006. Traditional medicine in central sahara: pharmacopoeia of tassili N'ajjer. *J. Ethnopharmacol.* 105, 358–367.
- Han, L.-T., Fang, Y., Li, M.-M., Yang, H.-B., Huang, F., 2013. The antitumor effects of triterpenoid saponins from the *Anemone flaccida* and the underlying mechanism. *Evid. Based Complement. Altern. Med.* <http://dx.doi.org/10.1155/2013/517931>.
- Hussain, A., Zia, M., Mirza, B., 2007. Cytotoxic and antitumor potential of *Fagonia cretica* L. *Turk. J. Biol.* 31, 19–24.
- Khalik, S.A., Miyase, T., El-Ashaal, H.A., Melek, F., 2000. Triterpenoid saponins from *Fagonia cretica*. *Phytochemistry* 54, 853–859.
- Khattak, K.F., 2012. Microbiological quality assessment of commercially available medicinal plants in Peshawar city. *Pak. Pak. J. Bot.* 44, 1203–1208.
- Lee, Y., Jung, J.-C., Ali, Z., Khan, I.A., Oh, S., 2012. Anti-inflammatory effect of triterpene saponins isolated from blue cohosh (*Caulophyllum thalictroides*). *Evid. Based Complement. Altern. Med.* 2012 <http://dx.doi.org/10.1155/2012/798192>.
- Liu, D., Zhen, W., Yang, Z., Carter, J.D., Si, H., Reynolds, K.A., 2006. Genistein acutely stimulates insulin secretion in pancreatic beta-cells through a cAMP-dependent protein kinase pathway. *Diabetes* 55, 1043–1050.
- Lunga, P.K., Qin, X.-J., Yang, X.W., Kuai, J.-R., Du, Z.Z., Gatsing, D., 2014. Antimicrobial steroidal saponin and oleanane-type triterpenoid saponins from *Paulinia pinnata*. *BMC Complement. Altern. Med.* 14, 369 (1–7).
- Luo, J.-G., Nie, W., Kong, L.-Y., 2011. Three new sulfated triterpenoids from the roots of *Gypsophila pacifica*. *J. Asian Nat. Prod. Res.* 13, 529–533.
- Mahmood, A., Qureshi, R.A., Mahmood, A., Sangi, Y., Shaheen, H., Ahmad, I., Nawaz, Z., 2011. Ethnobotanical survey of common medicinal plants used by people of district Mirpur, AJK, Pakistan. *J. Med. Plant Res.* 5, 4493–4498.
- Miyakoshi, M., Isoda, S., Sato, H., Hirai, Y., Shoji, J., Ida, Y., 1997. 3 α -Hydroxy-oleanene type triterpene glycosyl esters from leaves of *Acanthopanax spinosus*. *Phytochemistry* 46, 1255–1259.
- Miyase, T., Melek, F., El-Gindi, O., Abdel-Khalik, S., El-Gindi, M., Haggag, M., Hilal, S., 1996. Saponins from *Fagonia arabica*. *Phytochemistry* 41, 1175–1179.
- Nagaraj, D.S., Venkateswarlu, B., 2013. Antipyretic effect of aqueous extract of *Fagonia cretica* L. whole plant on brewer's yeast induced pyrexia in wistar rats. *Int. J. Pharmacol. Toxicol.* 3, 39–42.
- Ohno, T., Kato, N., Ishii, C., Shimizu, M., Ito, Y., Tomono, S., Kawazu, S., 1993. Genistein augments cyclic adenosine 3',5'-monophosphate (cAMP) accumulation and insulin release in MIN6 cells. *Endocr. Res.* 19, 273–285.
- Perrone, A., Masullo, M., Bassarello, C., Hamed, A.I., Belisario, M.A., Pizzi, C., Piacente, S., 2007. Sulfated triterpene derivatives from *Fagonia arabica*. *J. Nat. Prod.* 70, 584–588.
- Sajid, B., Alia, E., Rizwana, K., Uzma, S., Alamgeer, H.M., 2011. Phytochemical screening and antimicrobial activity of *Fagonia cretica* plant extracts against selected microbes. *J. Pharm. Res.* 4, 962–963.
- Saleem, S., Jafri, L., ul Haq, I., Chang, L.C., Calderwood, D., Green, B.D., Mirza, B., 2014. Plants *Fagonia cretica* L. and *Hedera nepalensis* K. Koch contain natural compounds with potent dipeptidyl peptidase-4 (DPP-4) inhibitory activity. *J. Ethnopharmacol.* 156, 26–32.
- Satpute, R.M., Kashyap, R.S., Deopujari, J.Y., Purohit, H.J., Taori, G.M., Dagnawala, H.F., 2009. Protection of PC12 cells from chemical ischemia induced oxidative stress by *Fagonia arabica*. *Food Chem. Toxicol.* 47, 2689–2695.
- Seyal, A., Awan, H., Tareen, S., 2013. Can we really treat thalassemia major? *Proc. Pak. Acad. Sci.* 50, 315–325.
- Shaker, K., Al Jubiri, S., El-Hady, F.A., Al-Sehemi, A., 2013. New compounds from *Bassia muricata* and *Fagonia indica*. *Int. J. Pharm. Sci. Res.* 23, 231–236.
- Shaker, K.H., Bernhardt, M., Elgamal, M.H.A., Seifert, K., 1999. Triterpenoid saponins from *Fagonia indica*. *Phytochemistry* 51, 1049–1053.
- Shaker, K.H., Bernhardt, M., Elgamal, M.H.A., Seifert, K., 2000. Sulfonated triterpenoid saponins from *Fagonia indica*. *Z. Naturforsch. C* 55, 520–523.
- Sharma, K.R., Adhikari, A., Hafizur, R.M., Hameed, A., Raza, S.A., Kalauni, S.K., Miyazaki, J.I., Choudhary, M.I., 2015. Potent insulin secretagogue from *Scoparia dulcis* linn of nepalese origin. *Phytother. Res.* 29, 1672–1675.
- Siddiqui, B.S., Hasan, M., Mairaj, F., Mehmood, I., Hafizur, R.M., Hameed, A., Shinwari, Z.K., 2014. Two new compounds from the aerial parts of *Bergenia himalaica* Boriss and their anti-hyperglycemic effect in streptozotocin-nicotinamide induced diabetic rats. *J. Ethnopharmacol.* 152, 561–567.
- Thetwar, L., Seema, A.S.T., Augor, M., Tandon, R., Deshmukh, N., 2006. Antimicrobial efficacy of methanolic extracts of *Fagonia cretica*. *Asian J. Chem.* 18, 743.
- Vetterli, L., Brun, T., Giovannoni, L., Bosco, D., Maechler, P., 2011. Resveratrol potentiates glucose-stimulated insulin secretion in INS-1E beta-cells and human islets through a SIRT1-dependent mechanism. *J. Biol. Chem.* 286, 6049–6060.
- Waheed, A., Barker, J., Barton, S.J., Owen, C.P., Ahmed, S., Carew, M.A., 2012. A novel steroidal saponin glycoside from *Fagonia indica* induces cell-selective apoptosis or necrosis in cancer cells. *Eur. J. Pharm. Sci.* 47, 464–473.
- Xiang, T., Tezuka, Y., Wu, L.-J., Banskota, A.H., Kadota, S., 2000. Saponins from *Lonicera bournei*. *Phytochemistry* 54, 795–799.